Universal front-end gain control aids robust combinatorial odor coding in naturalistic environments

Nirag Kadakia[a] **and Thierry Emonet**[a,b]

[a]Department of Molecular, Cellular, and Developmental Biology; [b]Department of Physics, Yale University, New Haven, CT 06511

This manuscript was compiled on October 4, 2018

Odor identity is encoded by spatiotemporal patterns of activity in olfactory receptor neurons (ORNs). In natural odor environments, the intensity and timecales of odor signals can span several orders of magnitude, and odors can mix with one another, potentially scrambling these combinatorial odor codes. The recent characterization of an odor- and ORN-independent adaptive scaling law in the *Drosophila* olfactory periphery – ORN gain scales inversely with odor concentration according to the Weber-Fechner law of psychophysics – may help preserve these neural representations of odor identity despite these possible confounds. Here we test this hypothesis with a minimal model of signal transduction, ORN firing, and signal decoding. We find that this adaptive scaling helps maintain coding capacity and promotes reconstruction of odor identity from dynamic odor signals, even in the presence of background confounds and rapid intensity fluctuations. Combining ORN adaptation with downstream mechanisms, such as normalization and divergence in the *Drosphila* antennal lobe and mushroom body, reveals that front-end adaptation could be a significant contributor to the fidelity of odor coding and decoding in insects. Together, our results suggest that despite the broad overlap of ORN tuning curves, a mechanism of front-end adaptation, when endowed with universal Weber-Fechner scaling via the co-receptor Orco, may play a vital role in preserving representations of odor identity in naturalistic odor landscapes.

Odor coding | Sensory systems | Weber's Law | Olfactory receptor neurons | *Drosophila melanogaster*

Animals identify and discriminate odors using olfactory receptors (Ors) expressed in olfactory receptor neurons (ORNs) (1, 2). Individual ORNs, which typically express a single Or (2), respond to many odorants, while individual odorants activate many distinct ORNs (3–6). Odors are thus encoded by the combinatorial patterns of activity they elicit in the sensing periphery (3–5, 7–9), patterns then decoded downstream into behavioral response (10). Ethologically-relevant odors are often mixed with background ones (11) and intensity can vary widely and rapidly as odors are carried by the wind (12–16). How are odors recognized reliably despite these confounds? Various mechanisms have been reported. In *Drosophila melanogaster*, OR-odorant dose response curves exhibit similar Hill coefficients but distinct power-law distributed activation thresholds (4, 16, 17), which together with inhibitory odorants enhance coding capacity (4, 17, 18). In antennal lobe (AL) glomeruli, mutual lateral inhibition normalizes population response, helping to maintain the invariance of activity patterns (19, 20). Further downstream, sparse connectivity to the mushroom body (MB) helps maintain neural representations of odors, and facilitates compressed sensing decoding schemes (21–23). Finally, temporal features of neural response may contribute to concentration-invariant representations of odor identity (24–27).

Here we examine how short-time adaptation (time scale 250 ms) at the very front-end of the insect olfactory circuit contributes to the fidelity of odor encoding. Our theoretical study is motivated by the recent discovery of invariances in the response dynamics of ORNs expressing the co-receptor Orco (16, 28–30). While for some Or-odor combinations, ORN response can exhibit large differences, such as super-sustained responses (31) or specialized responses to danger signals (), for many Or-odor combinations the deconvolution of stimulus dynamics from neuron responses produces highly stereotyped filters (17, 32), insensitive to odor concentration, enabling ORNs to maintain response time independent of odor intensity (16, 32). These properties stem in part from an apparently receptor-invariant mechanism of ORN adaptation: gain varies inversely with mean odor concentration according to Weber-Fechner's Law of psychophysics (16, 29, 30, 33, 34). This relatively fast adaptation ($\sim$ 250 ms) can be traced to feedback mechanisms in odor transduction, upstream of ORN firing (16, 29, 30, 35), and the generality of the scaling law suggests it may be mediated not by odor- or OR-dependent differences, but by the highly conserved Orco co-receptor (28, 36–38).

While in a single channel system such as *E. coli* chemotaxis, adaptive feedback via Weber-Fechner's Law robustly maintains sensitivity over concentration changes (39), the implication for a multiple-channel system – which combines information from several sensors with overlapping receptive fields – is less straightforward. Here we combine a biophysical model of universal ORN adaptive response and neural firing with various sparse signal decoding frameworks to explore how ORN adaptation affects combinatorial coding and decoding of odor signals spanning varying degrees of intensity, molecular complexity, and temporal structure. We find that this adaptive mechanism promotes the accurate discrimination of weak odor signals from strong backgrounds of varying molecular complexity, both in static odor environments and in fluctuating ones. We also investigate our framework in the context of the primacy coding hypothesis – that odors are encoded

Significance Statement

In insect olfaction, odors are believed to be encoded by the distinct spatiotemporal patterns of activity they elicit in sensing neurons. Here, we investigate how these patterns would be maintained in naturalistic environments, where odor concentrations can vary rapidly, and where ethologically-relevant odors often mix with nuisance backgrounds. We show that a robust mechanism of response adaptation, Weber-Fechner's Law of perceived difference, which was recently observed in *Drosophila*, may play a vital role in maintaining these odor codes. While Weber-Fechner's Law is known to maintain sensitivity in single-channel systems such as bacterial chemotaxis, here we illustrate its general applicability to multi-channels systems in which responses may be broad and highly overlapping.

N.K. and T.E. conceived the project, analyzed the results, and wrote the manuscript. N.K. performed all calculations. T.E. supervised the project.

Authors declare no conflict of interest

[2]To whom correspondence should be addressed. E-mail: thierry.emonetyale.edu

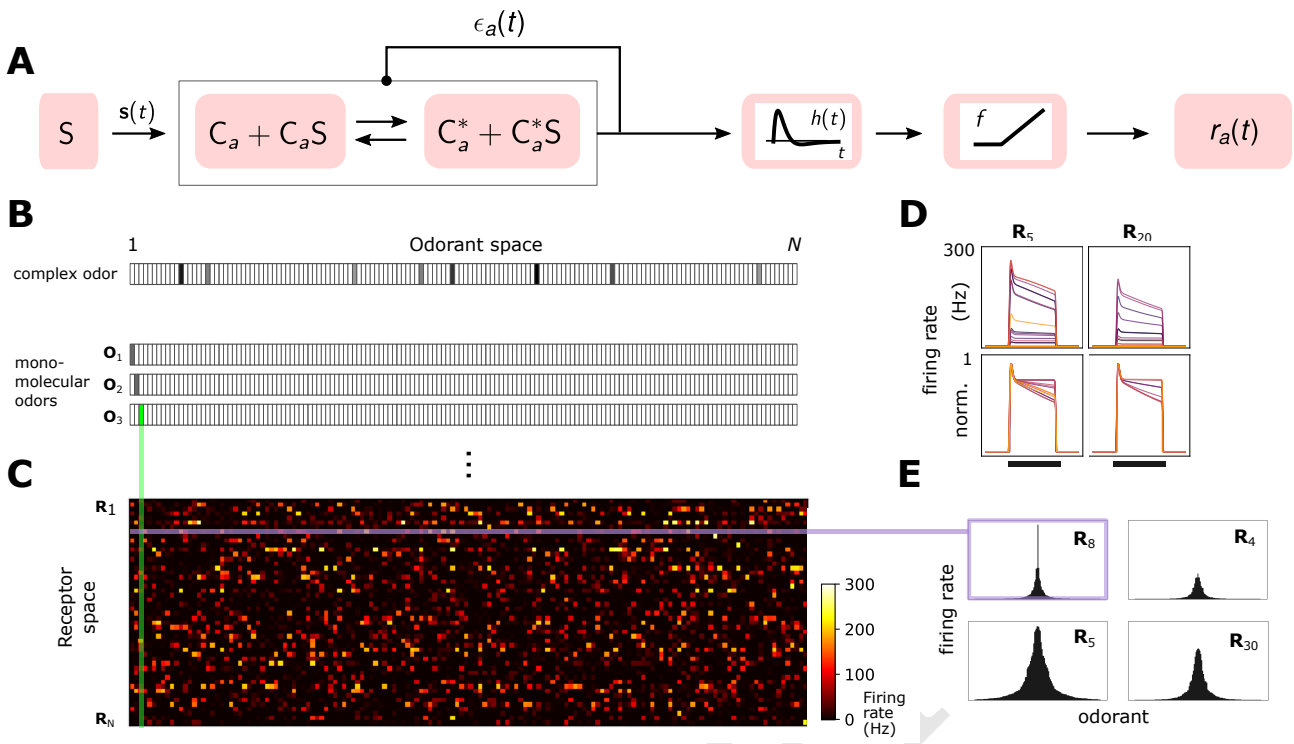

Fig. 1. **A** Odor binding model. Or/Orco complexes C_a bind odorant molecules s_i comprising stimuli S. These complexes can stochastically switch between inactive and active states, where the steady-state active fraction is determined by the complex free energy $\epsilon_a(t)$. The activity feeds back on to the free energies with timescale τ to pull the activity to a baseline level A_{a0}. ORN firing rates $r_a(t)$ are generated by passing $A_a(t)$ through a linear temporal filter $h(t)$ and a nonlinear thresholding function f. **B** Odor mixtures are represented by N-dimensional vectors $\mathbf{s}$, whose components s_i are the concentrations of the individual molecular constituents of $\mathbf{s}$. **C** The steady state firing response of 50 ORNs to the 150-possible monomolecular odors $\mathbf{s} = s_i$, given power-law distributed K_{ai}^* (17). **D** Temporal responses of two representative ORNs in response to a step stimulus, for several monomolecular odorants (colors); absolute firing rate (top row) and normalized rates (bottom row). **E** Representative ORN tuning curves, generated by ordering the responses within a single row of the response matrix in C. Tuning curves are diverse, mimicking measured responses (4).

entirely by the few earliest responding ORNs (27, 40), finding that primacy coding is both consistent with and enhanced by front-end adaptation.

Results

Model of ORN sensing repertoire. We consider a repertoire of $M = 50$ ORN types modeled using a simple extension of a minimal model of odor-to-ORN firing (16) that reproduces the Weber-Fechner adaptation and firing rate dynamics measured in individual *Drosophila* ORNs in response to Gaussian and naturalistic signals. Within ORNs of type $a = 1, ..., M$, Or-Orco complexes form non-selective cation channels (Fig. 1a) that stochastically switch between active and inactive states, while simultaneously binding to odorants i with dissociation constants, K_{ia}^* and K_{ia}, respectively (16, 35). Assuming these processes are faster than other reactions in the signaling pathway, the quasi-steady state active fraction A_a of channels in ORNs of type a is (Methods):

$$A_a(t) = \left(1 + e^{\epsilon_a(t)} \frac{1 + \sum_i^N s_i(t)/K_{ai}}{1 + \sum_i^N s_i(t)/K_{ai}^*}\right)^{-1}. \qquad [1]$$

$s_i(t)$ are the time-dependent concentrations of the individual monomolecular components of the odor signal $\mathbf{s}(\mathbf{t})$ at time t, and $N = 150$ is the size of the molecular odorant space (Fig. 1b). Inward currents elicited by activating Or-Orco channels eventually result in a negative feedback onto $A_a(t)$ (16, 30, 35):

$$\tau \frac{d\epsilon_a(t)}{dt} = A_{a0} - A_a(t). \qquad [2]$$

Here τ is the adaptation time and $\epsilon_a(t)$ is the free energy change due to modifications of the Or-Orco complexes by the short-term adaptation mechanism, which we assume is limited to a finite range $\epsilon_{\mathrm{L},a} < \epsilon_a(t) < \epsilon_{\mathrm{H},a}$ (16). Firing rate is minimally modeled by filtering the activity $A_a(t)$ with the double exponential filter $h(t)$ and rectifying nonlinearity f (Methods and (16)):

$$r_a(t) = f\left(h \otimes A_a(t)\right). \qquad [3]$$

Here, $\otimes$ represents convolution. When deconvolved from stimulus dynamics, the shapes of the temporal kernels of *Drosophila* ORNs that express Orco are largely receptor and odor independent (16, 17, 32). Moreover, adaptation is not intrinsic to the receptor (35). Accordingly, τ, $h(t)$ and f are assumed independent of receptor and odorant identities.

We assume that the lower cutoffs $\epsilon_{\mathrm{L},a}$ are receptor-dependent and choose them from a normal distribution. This variability ensures that ORNs are activated above quiescence (around 5 Hz) at distinct stimulus levels (16, 32). Diversity among odor-ORN responses mainly arises from the distribution of chemical dissociation constants. For simplicity we only consider agonists, i.e. $K_{ia}^* > K_{ia}$ but the analysis can easily be extended to include inhibitory odorants, which increases coding capacity (18). We choose the dissociation constants from a power law distribution ($\alpha = 0.35$) recently found across ORN-odor pairs in *Drosophila* larvae. For a handful of ORNs

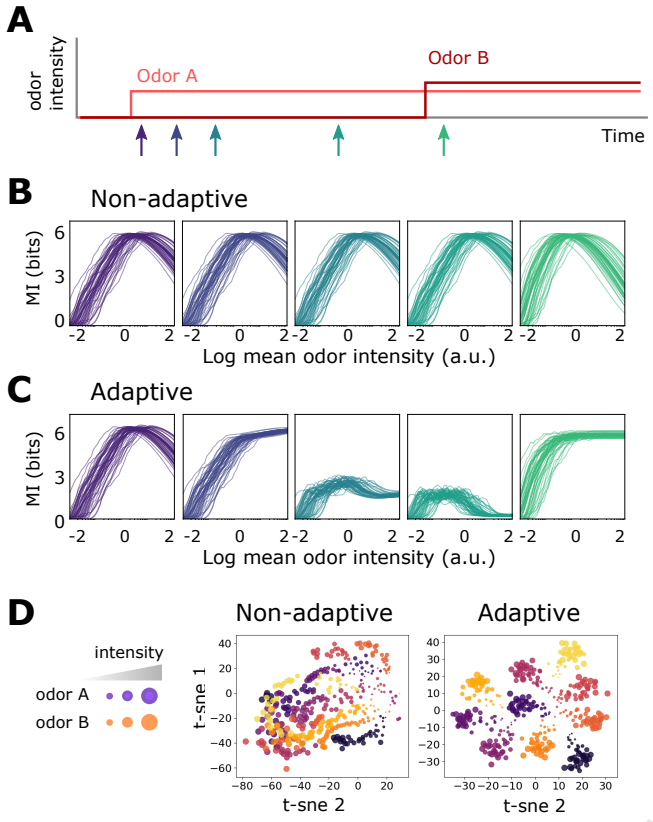

Fig. 2. Front-end adaptation maintains information capacity and representations of odor identity across changes in intensity. **A** Step of odor A is followed by a step of odor B at a later time t_B, where $t_B \gg \tau$. Odor A and B have similar intensities. **B** Evolution of mutual information (MI) between odor signals and ORN response, in the non-adaptive system, as a function of relative odor concentration. Thin lines are the MI contained in individual ORNs; heavy line is the average. MI is plotted at times of order of τ following t_A (purple; purple-blue), right before t_B (blue-green), and shortly after t_B (green). **C** Same as (B), for the adaptive system. **D** Abstract representation of ORN responses in reduced dimensions.

we choose a very small value for one of the K^*_{ai} to mimic high responders to private odorants relevant to innate responses. We checked that adding these private odors does not affect the general findings.

While this phenomenological model could be extended to include further details – e.g. we could relax the quasi-steady-state assumption in Eq. 1 and use a more complex model for the firing rate (16) – this minimally-parameterized form captures the key dynamical properties of Orco-expressing ORNs relevant to our study: receptor-independent adaptation (35) with universal Weber-Fechner scaling (16, 17, 29, 30) that maintains response time independent of mean stimulus intensity (16, 32), and diversity of both steady state tuning curves (4), as well as temporal firing patterns (24–26) in response to panels of monomolecular odorants (Fig. 1d-1e).

Concentration-invariant preservation of coding capacity. To investigate how front-end adaptation affects encoding capacity, we calculate the mutual information (MI) between odor signal $\mathbf{s} = \mathbf{s}_A + \mathbf{s}_B$ and response $\mathbf{r}$ as a function of signal intensity, with and without adaptation. A step of odor A, $\mathbf{s}_A$, turns on at time t_A and a step of odor B, $\mathbf{s}_B$ turns on at some later time t_B (Fig. 2a). Both odors have similar intensities. In the non-adaptive case, MI peaks around the region of maximum sensitivity ($\sim 10^2$ a.u.) after t_A (Fig. 2b). The adaptive system mimics the non-adaptive system at t_A, before adaptation has kicked in (Fig. 2c). In time, adaptation causes the sensitivity to decrease, and the mutual information peak shifts to higher concentrations. Eventually, all ORNS are firing at adapted baseline and mutual information is mostly eliminated. However, having now adjusted its regime of maximum sensitivity to the presence of odor A, the system can respond appropriately to odor B: the MI at t_B is nearly 6 bits across 3 decades of concentration.

We expect that preservation of information capacity helps maintain odor identity. We visualize this by projecting the 50-dimensional ORN response $\mathbf{r}$ to a lower two-dimensional space using t-distributed stochastic neighbor embedding (t-SNE) (41). Testing this both for a smaller (Fig. 2d) and larger (SI) odor repertoire, odors cluster by identity in the adaptive system, while in the non-adaptive system, representations mix among their identity and concentration. This suggests that universal front-end adaptative feedback helps preserves odor identities within the ensemble of ORN response.

Front-end adaptation enhances odor discrimination in complex environments. How well does the preservation of coding capacity translate to better signal reconstruction? One potentially complicating factor is the disparity between sensor dimension and stimulus dimension: while *Drosophila* only express ~ 60 olfactory receptor genes (42), the space of odorants is far greater (23). However, many naturally-occurring odors are comprised of a small subset of odorants, which is suggestive as mathematical results in compressed sensing guarantee their reconstruction, assuming a sufficiently random response (23, 43–45). There is no direct evidence that a compressed decoding framework is implemented in the *Drosophila* olfactory circuit (46). Here we used this framework as a mathematical tool to quantify how front-end adaptation potentially affects odor decoding. We later verify our conclusions with other classification techniques that make use of the known architecture of the olfactory system.

To incorporate the linear framework of compressed sensing, we treat the nonlinear odor encoding exactly but approximate the decoding to first order. Odors $\mathbf{s}$ are assumed sparse, with $K \ll N$ nonzero components s_i with mean concentration s_0. We first examine how foreground odors are recognized when mixed with background odors, quantifying decoding accuracy as the percentage of odors correctly decoded within some tolerance (Fig. 3a). Without adaptation, detection accuracy for concentrations is maintained within the range of receptor sensitivity, for a simple, weak background. However, accuracy is virtually eliminated as background complexity K and intensity rise (Fig. 3b). The range of the sensitivity is higher in the adaptive system, and it is substantially more robust across changes in molecular complexity and intensity of the background odors (Fig. 3c).

In realistic odor environments, the concentration and duration of individual odor whiffs vary widely (14), and we wondered how well a front-end adaptation mechanism with a single timescale τ could promote whiff detection in such environments. As inputs to our coding/decoding framework we apply a naturalistic stimulus intensity recorded using a photo-ionization detector (16) (Fig. 3d) to which we randomly assign sparse identities from the N-dimensional odorant space. To mimic background confounds, we combine these signals with static odor backgrounds, and then calculate the percentage of decoded whiffs (purple bars in Fig. 3d). We also assume a finite length of short-term memory: detected odor signals are only retained τ_F seconds in the immediate past (Methods). Without ORN adaptation, sufficiently strong backgrounds eliminate the ability to reconstruct the identity of individual odor whiffs, irrespective of the complexity of either the foreground or background odor (Fig. 3e, green lines). In

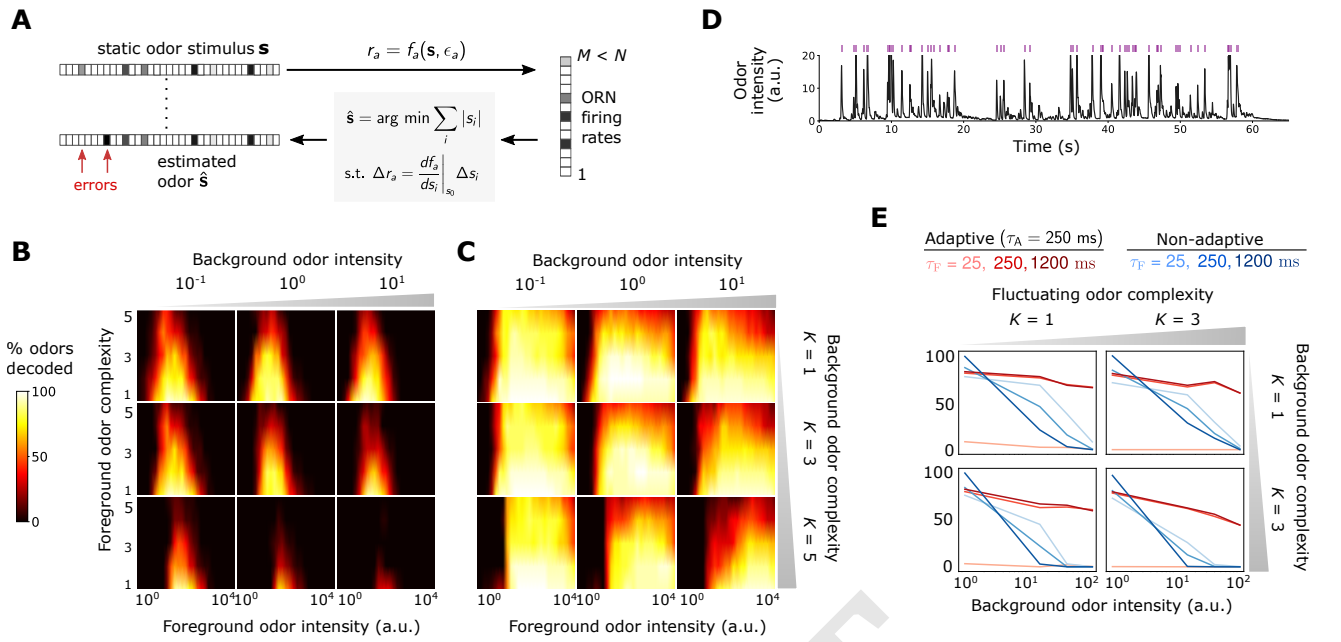

Fig. 3. Front-end adaptation promotes accurate sparse odor decoding in static and naturalistic odor environments. **A** Odor stimuli produce ORN responses via odor-binding and activation and firing machinery, as described by Eqs. 1-3. Odors are then decoded using compressed sensing by linearizing around a background s_0 and minimizing the constrained L_1 norm of the odor signal. Odors are assumed sparse, with K nonzero components, $K \ll N$. **B** Decoding accuracy of foreground odors in the presence of background odors, without front-end adaptation. Individual heatmaps show the decoding accuracy of the foreground odor as a function of its intensity and complexity; plots are arrayed by background odor intensity (column-wise) and complexity (row-wise). Odors are considered accurately decoded if the K sparse components are estimated within 25% and the components not in the mixture are estimated below 10% of s_0. **C** Same as (B), for the adaptive system. **D** Recorded trace of naturalistic odor signal; whiffs (signal > 5 a.u.) demarcated by purple bars. This signal is added to static backgrounds of different intensities and complexities, which is then decoded in time. **E** Individual plots show the percent of accurately decoded odor whiffs as a function of background odor intensity, for the non-adaptive (blue) and adaptive (red) systems, for different t_F (line shades). Plots are arrayed by the complexity of the naturalistic signal (column-wise) and the complexity of the background odor (row-wise)

the adaptive system, this is substantially mitigated (red lines in Fig. 3e), as long as the memory duration τ_F is on the same order as the adaptation timescale τ (darker red lines).

Front-end adaptation enhances primacy coding. The primacy coding hypothesis posits that odor identity is encoded by the set (but not temporal order) of the p earliest responding glomeruli/ORN types, known as primacy set of order p (27). If the activation order of ORNs were invariant to the strength of an odor step or pulse, primacy sets would in principle form concentration-invariant representation of odor identity. Though our coding framework uses the full ORN ensemble in signal reconstruction, some of these ORN responses may contain redundant information, and a smaller primacy subset may suffice. To examine this relationship, we apply our model to a sigmoidal stimulus that rises to half-max in 50 ms, calculating decoding accuracy in time. Since ORNs activate sequentially, the primacy set is defined by the ORN subset active when the odor is accurately decoded. For simple odors, a limited set of earliest responding neurons fully accounts for the odor identity ($K = 1, 3, 5$ plots in Fig. 4a), in agreement with primacy coding. As expected for more complex odor mixtures, the full repertoire is required for accurate decoding ($K = 7, 9$ plots in Fig. 4a). Primacy coding also predicts that for stronger stimuli, responses occur earlier in time, since the primacy set is realized quicker, which our framework replicates (SI).

Beyond mere consistency, however, front-end adaptation might also enhance primacy coding in different environmental conditions, such as background odors, which could scramble primacy sets. To investigate this, we calculated the primacy sets for 1000 sparse odor mixtures atop various static backgrounds. We find that primacy sets for these mixtures are preserved across different background concentrations, for all but the smallest primacy orders (Fig. 4c). This suggests that front-end adaptation may play a central role in reinforcing primacy codes across differing environmental conditions.

Contribution of front-end adaptation for odor recognition within the *Drosophila* olfactory circuit. Signal transformations in the sensing periphery are propagated through the remainder of the olfactory circuit. How does front-end adaptation interact with these subsequent neural transformations? ORNs expressing the same OR converge to a unique AL glomerulus, where they receive lateral inhibition from other glomeruli (19, 47). This inhibition implements a type of divisive gain control (20), normalizing the activity of output projections neurons, which then synapse onto a large number of Kenyon cells (KCs) in the mushroom body. To investigate how odor representations are affected by interactions between front-end ORN adaptation and this lateral inhibition and synaptic divergence, we extended our ORN encoding model by adding uniglomerular connections from ORNs to the antennal lobe, followed by sparse, divergent connections to 2500 KCs (21, 22, 48). Inhibition was modeled via divisive normalization, with parameters chosen according to experiment (20). We quantified decoding accuracy by training and testing a binary classifier on the KC activity output of sparse odors of distinct intensity and identity, randomly categorized as appetitive or aversive. Odor signals of the same identity but differing intensity were assigned the same valence. We trained the classifier on N_{ID} sparse odor identities at intensities chosen randomly over 4 orders of magnitude, then tested the classifier accuracy on the same odor identities but of differing concentrations.

Classification accuracy degrades to chance level as N_{ID} becomes very large (Fig. 5a). When acting alone, either di-

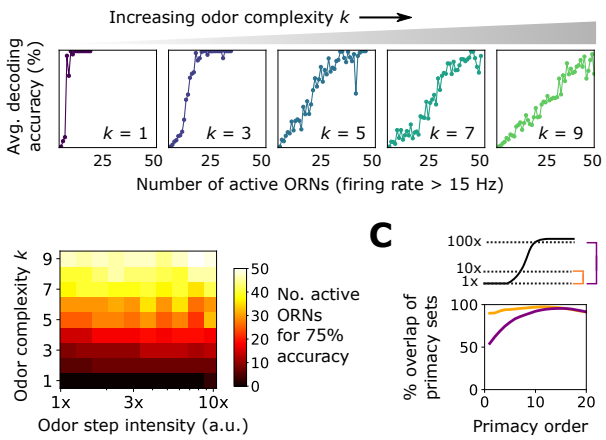

Fig. 4. **A** Decoding accuracy as a function of the number of active ORNs (firing rate $>$ 15 Hz), for different odor complexities. The primacy set consists of those ORNs required to be active for accurate decoding; the set size grows with odor complexity. **B** Number of active ORNs required to fully decode odor signals of varying odor intensity and complexity. **C** Primacy sets for a step signal in the presence of different background intensities are almost identical for all but the smallest primacy orders ($p \gtrapprox 5$). Yellow: overlap of the primacy sets for step signal when placed atop a weak (1x) vs. a medium (10x) background; purple: overlap of primacy sets for step signal atop weak vs. strong (100x) backgrounds.

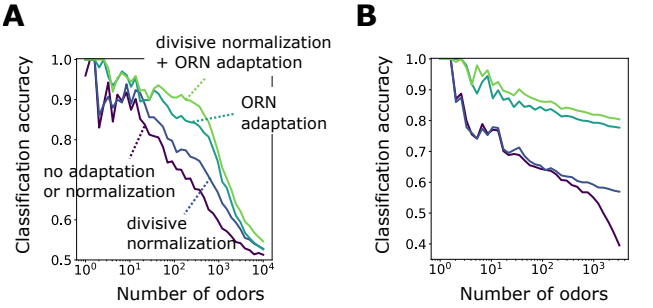

Fig. 5. **A** Accuracy of binary classification by odor valence, as a function of the number of distinct odor identities classified by the trained network (concentrations span 4 orders of magnitude), in systems with only ORN adaptation, only divisive normalization, both or neither. **B** Same as (A) but now classifying odors by identity.

visive normalization or ORN adaptation can help, although the effect of ORN adaptation is stronger. When both are active, accuracy improves further, suggesting that these distinct adaptive transformations may act jointly at different stages of neural processing in preserving representations of odor identity. Interestingly, if we train the classifier to distinguish odors by their distinct identity, rather than valence, we find that the benefits conferred by divisive normalization do not appear until N_{ID} is substantial, with accuracy below 65% for $N_{ID} > 50$ (Fig. 5b). On the other hand, with ORN adaptation accuracy remains above 85% for more than 1000 odor identities, strongly implicating front-end adaptation as a key player in maintaining odor identity representations, before they are further processed downstream.

Discussion

We investigated the theoretical implications the Weber-Fechner input gain control (16, 29, 30) and activity-dependent adaptation (16, 32, 35) observed in *Drosophila* olfactory receptor neurons and found that they contribute to preserving neural representations of odor identity within the olfactory pathway. Our conclusions rely on both a compressed sensing scheme that fully reconstructs odor signals from neural response, as well as classification algorithms that categorize odors by identity or valence. We find that such input gain control enhances the coding capacity of ensemble ORN response, helping maintain representations of odor identity independent of intensity (Figs. 1 and 2). It acts jointly with normalization in the AL to aid the discrimination of naturalistic odor signals from static backgrounds, implicating the importance of signal transformations at multiple steps in the olfactory circuit (Figs. 3 and 5). In the context of primacy coding – that signals are encoded by the earliest activating glomeruli – we find that front-end adaptation enhances primacy coding by maintaining primacy sets amid background confounds (Fig. 4).

While our model incorporates many observed features of *Drosphila* olfactory sensing – Weber-Law adaptation, power-law distributed receptor affinities, temporal filter invariance, connectivity topologies – it is a minimal model. We considered only one of the olfactory receptor families expressed in the fly antenna () and considered only short-time adaptation (16, 32, 35), adaptation at ??? a(synapse etc...) as well as orcor mediated long-term adaptation havbe also been observed and may enbale anumals to tune the contrast between odors of interest depending on longer timescale accroding to needs , e.g. being hungry. Our study assumes such adaptation have taken place We neglected the role of inhibitory odorants, and suspect they would boost coding capacity and aid signal reconstruction as explored previously (30). We also neglected coupling between neighboring ORNs within the same sensillum (49): odorants inhibitory for one ORN but excitatory for the other could affect coding capacity by exploiting response bidirectionality.

Previous studies in the *Drosophila* olfactory circuit have characterized various response features that preserve combinatorial codes. Lateral inhibition helps tame saturation and boost weak signals (20). ORNs exhibiting both excitatory and inhibitory responses to odorants can increase coding capacity by exploiting response bidirectionality (18). In vertebrates, antagonism among odorants may help maintain response sparsity (50). Finally, in both vertebrates and insects, the degree of connectivity to either the olfactory bulb or mushroom body (each KC receives connections from only ∼6 AL glomeruli) may be precisely tuned to optimize the system's capacity to learn associations (22). Here, we find that some of these downstream features (lateral inhibition and sparse connectivity) appear to act in concert with front-end dynamic adaptation in maintaining representations of odor identity.

Other studies have implicated the unique temporal patterns of neural response as signatures of odor identity (24–26, 51). ORN and projection neuron time traces form distinct trajectories in low-dimensional projections, and cluster by odor identity, much as we have found here (Fig. 2b). In our framework, temporal coding is implicit: Because the strength of feedback onto Or/Orco activation depends on an ORN's unique response characteristics, odor signals are naturally formatted into temporal patterns that are both odor- and ORN-specific – despite the universality of τ (Fig. 1e). Further, the short forgetting timescales, $\tau_F \sim \tau \sim 250$ ms, suggest that only brief time windows are needed for accurate odor identification, consistent with previous findings (24).

In living systems, sensory adaptation ensures that responses remain in regimes of maximum sensitivity, increasing their effective dynamic range (52–55). Doing so requires matching sensory response to attributes of the environment, either by adapting to specific stimuli or to stimuli statistics (52). In a single-channel system such as bacterial chemotaxis, information capacity is increased by matching the midpoint of the

nonlinear dose-response curve, where sensitivity is highest, to mean ligand concentration (56). This is enacted in a robust and dynamic way, through a feedback loop from the activity output of the pathway onto proteins dictating receptor sensitivity (39, 57). We hypothesize that an analogous feedback loop exists in olfactory receptor neurons, from Orco-mediated Or channel activity onto the free energy of receptor activation (16). This mechanism appears to act identically across ORNs, and because olfactory tuning curves are highly overlapping, raises questions about its efficacy in complex environments: adaptation to one odor could adversely affect identification of a new odor if the latter excites some but not all of the same ORNs. Our results show that this general feedback, operating at a single timescale, indeed helps preserve combinatorial representations of odor identity, despite these broad overlaps.

Methods

The odor-binding and Or/Orco activation dynamics are assumed competitive (complexes bind at most one odorant), described for each complex a by a 2(N+1)-state system $\{C_a, C_a^*, C_a\text{-}s_i, C_a^*\text{-}s_i\}$ with rate equations $C_a \rightleftharpoons s_i\text{-}C_a$, $C_a^* \rightleftharpoons s_i\text{-}C_a^*$, $C_a \rightleftharpoons C_a^*$, and $C_a\text{-}s_i \rightleftharpoons C_a^*\text{-}s_i$. The first two of these describe the odor binding dynamics, with equilibrium constants K_{ai} and K_{ai}^*, respectively. The latter two describe activation, with rate constants $w_{a,\pm} \propto (1+\exp(\pm\epsilon_a))$ and $w_{a,\pm}^* \propto (1+\exp(\pm\epsilon_{a,i}))$, respectively. For ORN firing, $h(t)$ is bi-lobed (32): $h(t) = C_f(f_X(t;\alpha_1,\tau_1) - f_X(t;\alpha_2,\tau_2))$, $C_f = 190$, $\alpha_1 = 2$, $\alpha_2 = 3$, $\tau_1 = 0.006$, and $\tau_2 = 0.008$, where f_X is the pdf of Gamma(α_i, $1/\tau_i$). Nonlinearity f is modeled as a linear rectifier with 5 Hz threshold.

Mutual information was calculated from 1000 randomly chosen sparse odor identities ($K = 4$ for both odor A and odor B), with noise $\sigma \sim \mathcal{N}(0, 1\text{e-}3)$ added to A_a. For t-SNE dimensionality reduction, ORN responses were generated for 10 sparse odors ($K = 5$) at 40 concentrations spanning 4 decades. These odors were mixed with random sparse background odors ($K = 2$) of similar magnitude; in the adaptive system, the activity level given by this background sets ϵ_a via the fixed point of Eq. 2.

For compressed sensing decoding, sparse components s_i are chosen as $s_i = s_0 + \Delta s_i$ where s_0 is set as the center of linearization and $\Delta s_i \sim \mathcal{N}(s_0/3, s_0/9)$. Reconstructed signal components $\hat{s}_i = s_0 + \Delta s_i$ are computed by minimizing $\sum_i |\Delta s_i|$ subject to $\Delta r_a = \sum_i dr_a/ds_i\big|_{s_0} \Delta s_i$ where $\Delta r_a = r_a(\mathbf{s}) - r_a(s_0)$ are the "excess" ORN firing rates about the linearization point. For static stimuli, ϵ_a equals the fixed point of Eq. 2; for fluctuating stimuli, ϵ_a is updated in time by continuously integrating $r_a(t)$, via Eqs. 2 and 3; thus, only knowledge of $r_a(t)$ is needed by the decoder.

For the network model, the AL-to-MB connectivity matrix $\mathbf{J}_1$, is chosen such that each KC connects pre-synaptically to 7 randomly chosen AL glomeruli (21, 22). These $Z = 2500$ KCs are connected by a matrix $\mathbf{J}_2$ to a readout layer of dimension Q, where $Q = 2$ for binary and $Q = N_{\mathrm{ID}}$ for multi-class classification. Both AL-to-MB and MB-to-readout connections are perceptron-type with rectified-linear thresholds. The weights of $\mathbf{J}_1$ and $\mathbf{J}_2$ are chosen randomly from $\sim \mathcal{N}(0, 1/\sqrt{7})$ and $\sim \mathcal{N}(0, 1/\sqrt{Z})$, respectively. Only the $\mathbf{J}_2$ and the MB-to-output thresholds are updated during supervised network training, via logistic regression (for binary classification) or its higher-dimensional generalization, the softmax cross entropy (for multi-class classification).

1. Couto A, Alenius M, Dickson BJ (2005) Molecular, anatomical, and functional organization of the drosophila olfactory system. *Current Biology* 15(17).
2. Buck L, Axel R (1991) A novel multigene family may encode odorant receptors: a molecular basis for odor recognition. *Cell* 65(1):175–187.
3. Friedrich RW, Korsching SI (1997) Combinatorial and chemotopic odorant coding in the zebrafish olfactory bulb visualized by optical imaging. *Neuron* 18(5):737–752.
4. Hallem E, Carlson J (2006) Coding of odors by a receptor repertoire. *Cell* 125(1):143–160.
5. Wang G, Carey AF, Carlson JR, Zwiebel LJ (2010) Molecular basis of odor coding in the malaria vector mosquito anopheles gambiae. *Proceedings of the National Academy of Sciences* 107(9):4418–4423.
6. Nara K, Saraiva LR, Ye X, Buck LB (2011) A large-scale analysis of odor coding in the olfactory epithelium. *Journal of Neuroscience* 31(25):9179–9191.
7. Malnic B, Hirono J, Sato T, Buck LB (1999) Combinatorial receptor codes for odors. *Cell* 96(5):713–723.
8. Hildebrand JG, Shepherd GM (1997) Mechanisms of olfactory discrimination: converging evidence for common principles across phyla. *Annual review of neuroscience* 20(1):595–631.
9. de Bruyne M, Foster K, Carlson JR (2001) Odor coding in the drosophila antenna. *Neuron* 30(2):537 – 552.
10. Wilson RI (2013) Early olfactory processing in *Drosophila*: mechanisms and principles. *Annual Review of Neuroscience* 36(1):217–241.
11. Renou M, Party V, Rouyar A, Anton S (2015) Olfactory signal coding in an odor background. *Biosystems* 136:35 – 45.
12. Murlis J (1992) Odor plumes and how insects use them. *Annual Review of Entymology* 37:505–532.
13. Weissburg M (2000) The fluid dynamical context of chemosensory behavior. *The Biological Bulletin* 198(2):188–202. PMID: 10786940.
14. Celani A, Villermaux E, Vergassola M (2014) Odor landscapes in turbulent environments. *Phys. Rev. X* 4(4):041015.
15. Cardé RT, Willis MA (2008) Navigational strategies used by insects to find distant, wind-borne sources of odor. *Journal of Chemical Ecology* 34(7):854–866.
16. Gorur-Shandilya S, Demir M, Long J, Clark DA, Emonet T (2017) Olfactory receptor neurons use gain control and complementary kinetics to encode intermittent odorant stimuli. *eLife* 6:e27670.
17. Si G, et al. (2017) Invariances in a combinatorial olfactory receptor code. *bioRxiv* p. 208538.
18. Cao LH, et al. (2017) Odor-evoked inhibition of olfactory sensory neurons drives olfactory perception in *Drosophila*. *Nature Communications* 8(1):1357.
19. Asahina K, Louis M, Piccinotti S, Vosshall L (2009) A circuit supporting concentration-invariant odor perception in *Drosophila*. *Journal of Biology* 8(1):9.
20. Olsen SR, Vikas B, Wilson RI (2010) Divisive normalization in olfactory population codes. *Neuron* 66:287–299.
21. Caron S, Ruta V, Abbott L, Axel R (2013) Random convergence of olfactory inputs in the *Drosophila* mushroom body. *Nature* 497(4774):113–117.
22. Litwin-Kumar A, Harris KD, Axel R, Sompolinsky H, Abbott L (2017) Optimal degrees of synaptic connectivity. *Neuron* 93(5):1153 – 1164.e7.
23. Krishnamurthy K, Hermundstad AM, Mora T, Walczak AM, Balasubramanian V (2017) Disorder and the neural representation of complex odors: smelling in the real world. *bioRxiv* doi:10.1101/160382.
24. Brown SL, Joseph J, Stopfer M (2005) Encoding a temporally structured stimulus with a temporally structured neural representation. *Nature Neuroscience* 8:1568–1576.
25. Raman B, Joseph J, Tang J, Stopfer M (2010) Temporally diverse firing patterns in olfactory receptor neurons underlie spatiotemporal neural codes for odors. *Journal of Neuroscience* 30(6):1994–2006.
26. Gupta N, Stopfer M (2014) A temporal channel for information in sparse sensory coding. *Neuron* pp. 2247–2256.
27. Wilson CD, Serrano GO, Koulakov AA, Rinberg D (2017) A primacy code for odor identity. *Nature Communications* 8(1):1477.
28. Larsson MC, et al. (2004) Or83b encodes a broadly expressed odorant receptor essential for drosophila olfaction. *Neuron* 43(5):703 – 714.
29. Cafaro J (2016) Multiple sites of adaptation lead to contrast encoding in the *Drosophila* olfactory system. *Physiological Reports* 4(4):e12762.
30. Cao LH, et al. (2016) Distinct signaling of *Drosophila* chemoreceptors in olfactory sensory neurons. *Proceedings of the National Academy of Sciences* 113(7):E902–E911.
31. Montague SA, Mathew D, Carlson JR (2011) Similar odorants elicit different behavioral and physiological responses, some supersustained. *Journal of Neuroscience* 31(21):7891–7899.
32. Martelli C, Carlson JR, Emonet T (2013) Intensity invariant dynamics and odor-specific latencies in olfactory receptor neuron response. *Journal of Neuroscience* 33(15):6285–6297.
33. Weber EH (1996) *EH Weber on the tactile senses*. (Psychology Press).
34. Fechner GT (1860) *Elemente der psychophysik*. (Breitkopf und Härtel).
35. Nagel K, Wilson R (2011) Biophysical mechanisms underlying olfactory receptor neuron dynamics. *Nature Neuroscience* 14:208–216.
36. Getahun MN, Olsson SB, Lavista-Llanos S, Hansson BS, Wicher D (2013) Insect odorant response sensitivity is tuned by metabotropically autoregulated olfactory receptors. *PLoS One* 8(3):e58889.
37. Getahun MN, et al. (2016) Intracellular regulation of the insect chemoreceptor complex impacts odour localization in flying insects. *Journal of Experimental Biology* 219(21):3428–3438.
38. Butterwick JA, et al. (2018) Cryo-em structure of the insect olfactory receptor orco. *Nature* 560:447–452.
39. Alon U, Surette M, N. B, Leibler S (1999) Robustness in bacterial chemotaxis. *Nature* 397:168–171.
40. Giaffar H, Rinberg D, Koulakov AA (2018) Primacy model and the evolution of the olfactory receptor repertoire. *biorxiv*.
41. van der Maaten L, Hinton G (2008) Visualizing high-dimensional data using t-sne. *Journal of Machine Learning Research* 9:2579–2605.
42. Vosshall LB, Wong AM, Axel R (2000) An olfactory sensory map in the fly brain. *Cell* 102(2):147 – 159.
43. Donoho D (2006) Compressed sensing. *IEEE Transactions on Information Theory* 52(4):1289–1306.
44. Candes E, Romberg J, Tao T (2006) Robust uncertainty principles: Exact signal reconstruction from highly incomplete frequency information. *IEEE Transactions on Information Theory* 52(2):489–509.
45. Ganguli S, Sompolinsky H (2012) Compressed sensing, sparsity, and dimensionality in neuronal information processing and data analysis. *Annual Review of Neuroscience* 35(1):485–508.
46. Pehlevan C, Genkin A, Chklovskii DB (2017) A clustering neural network model of insect olfaction in *2017 51st Asilomar Conference on Signals, Systems, and Computers*. pp. 593–600.
47. Olsen SR, Wilson RI (2008) Lateral presynaptic inhibition mediates gain control in an olfactory circuit. *Nature* 452:952–960.

48. Keene AC, Waddell S (2007) *Drosophila* olfactory memory: single genes to complex neural circuits. *Nature Reviews Neuroscience* 8:341–354.
49. Su CY, Menuz K, Reisert J, Carlson J (2012) Non-synaptic inhibition between grouped neurons in an olfactory circuit. *Nature* 492(7427):76–71.
50. Reddy G, Zak J, Vergassola M, Murthy VN (2017) Antagonism in olfactory receptor neurons and its implications for the perception of odor mixtures. *bioRxiv* p. 204354.
51. Gupta N, Stopfer M (2011) Insect olfactory coding and memory at multiple timescales. *Current Opinion in Neurobiology* 21:768–773.
52. Wark B, Lundstrom BN, Fairhall A (2007) Sensory adaptation. *Current Opinion in Neurobiology* 17(4):423–429.
53. Nagel KI, Doupe AJ (2006) Temporal processing and adaptation in the songbird auditory forebrain. *Neuron* 51(6):845 – 859.
54. Laughlin SB (1981) A simple coding procedure enhances a neuron's information capacity. *Zeitschrift für Naturforschung C* 36(9-10):910–912.
55. DeWeese M, Zador A (1998) Asymmetric dynamics in optimal variance adaptation. *Neural Computation* 10:1179–1202.
56. Nemenman I (2012) Information theory and adaptation in *Quantitative Biology: From Molecular to Cellular Systems*, ed. Wall ME. (CRC Press, USA), pp. 73–91.
57. Barkai N, Leibler S (1997) Robustness in simple biochemical networks. *Nature* 387:913–917.